Conference Record of IEEE Workshop on Measurement of Electrical Quantities in Pulse Power Systems II
5-7 March 1986, pp. 49-53
IEEE Dielectrics and Electrical Insulation Society
IEEE No. 86CH 2327-5

Sensor and Simulation Notes
Note 290
14 October 1985

SURFACE-CURRENT-DENSITY MEASUREMENTS VIA APERTURES

Y.-G. Chen, S. Lloyd and R. Crumley
Maxwell Laboratories, Inc., San Diego, CA

Carl E. Baum
Air Force Weapons Laboratory

and

D.V. Giri
Pro-Tech, 125 University Avenue, Berkeley, CA 94710

290

291

Abstract

This note addresses the problem of measuring the surface current densities on conducting surfaces. If the surface current density on one side is of interest, a sensing loop on the side of interest can yield accurate results. Also two loops, one on each side can give individual surface current densities on both sides, while the total current density equal to the sum of the surface current densities on the two sides can be measured by differencing the outputs of the two loops. However, in certain applications, the total-surface-current-density measurement is more easily performed by a single aperture. Some versions of such an aperture are discussed here.

Sensor and Simulation Notes
Note 290
14 October 1985

SURFACE-CURRENT-DENSITY MEASUREMENTS VIA APERTURES

Y.-G. Chen, S. Lloyd and R. Crumley
Maxwell Laboratories, Inc., San Diego, CA

Carl E. Baum
Air Force Weapons Laboratory

and

D.V. Giri
Pro-Tech, 125 University Avenue, Berkeley, CA 94710

Abstract

This note addresses the problem of measuring the surface current densities on conducting surfaces. If the surface current density on one side is of interest, a sensing loop on the side of interest can yield accurate results. Also two loops, one on each side can give individual surface current densities on both sides, while the total current density equal to the sum of the surface current densities on the two sides can be measured by differencing the outputs of the two loops. However, in certain applications, the total-surface-current-density measurement is more easily performed by a single aperture. Some versions of such an aperture are discussed here.

Contents

I. Introduction

In various electromagnetic applications, there exists a need for the measurement of surface current densities. Traditionally, such measurements are made with the use of sensing loops. The voltage induced in the loop which is the negative line integral of the electric field is proportional to the time rate of change of the magnetic flux. The tangential magnetic field $\vec{H}_1$ at a perfectly conducting surface S, as shown in figure 1.1 is easily related to the surface current density $\vec{J}_{s_1}$ according as

$$\vec{I}_{S_1} \times \vec{H}_1 = \vec{J}_{s_1} \quad , \quad \vec{H}_1 = -\vec{I}_{S_1} \times \vec{J}_{s_1} \tag{1.1}$$

where $\vec{I}_{S_1}$ is the unit normal pointing away from the side of interest denoted by subscript 1. This has successfully been implemented in the past [1,2 and 8], and several magnetic field sensors with varying sensitivities have been fabricated and widely used.

Note that in figure 1.1, the tangential magnetic field on the other side (side 2) is of no interest and does not influence the measurement on side 1. The integration contour C_ℓ for the electric field or the "loop" is indicated in figure 1.1 and the measured voltage $V(t)$ is given by

$$V_\ell(t) = -\oint_{C_\ell} \vec{E}_1(t)\cdot d\vec{\ell} = \frac{\partial \Phi_m(t)}{\partial t} = \vec{A}_{eq_\ell} \cdot \frac{\partial \vec{B}_1(t)}{\partial t} \tag{1.2}$$

where $\vec{E}_1$ is the electric field, Φ_m is the total magnetic flux, $\vec{A}_{eq_\ell}$ is the equivalent area of the loop and $\vec{B}_1$ is the magnetic flux density related to the tangential magnetic field via

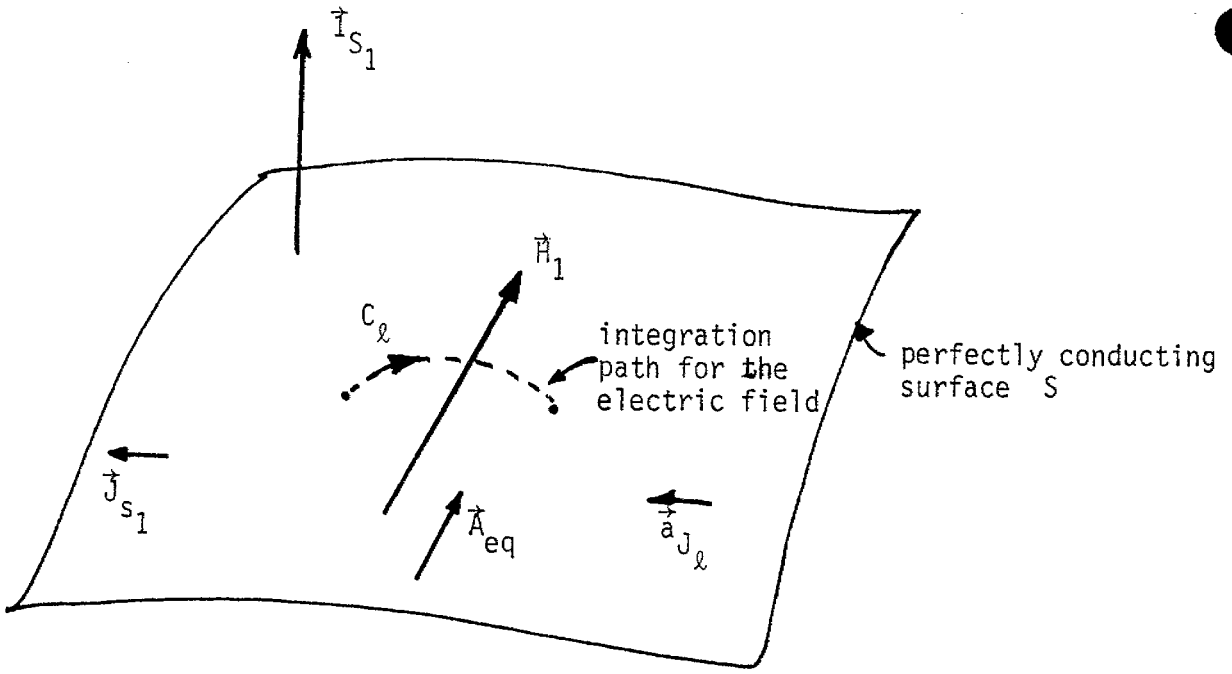

Figure 1.1 Measurement of surface magnetic fields with loops.

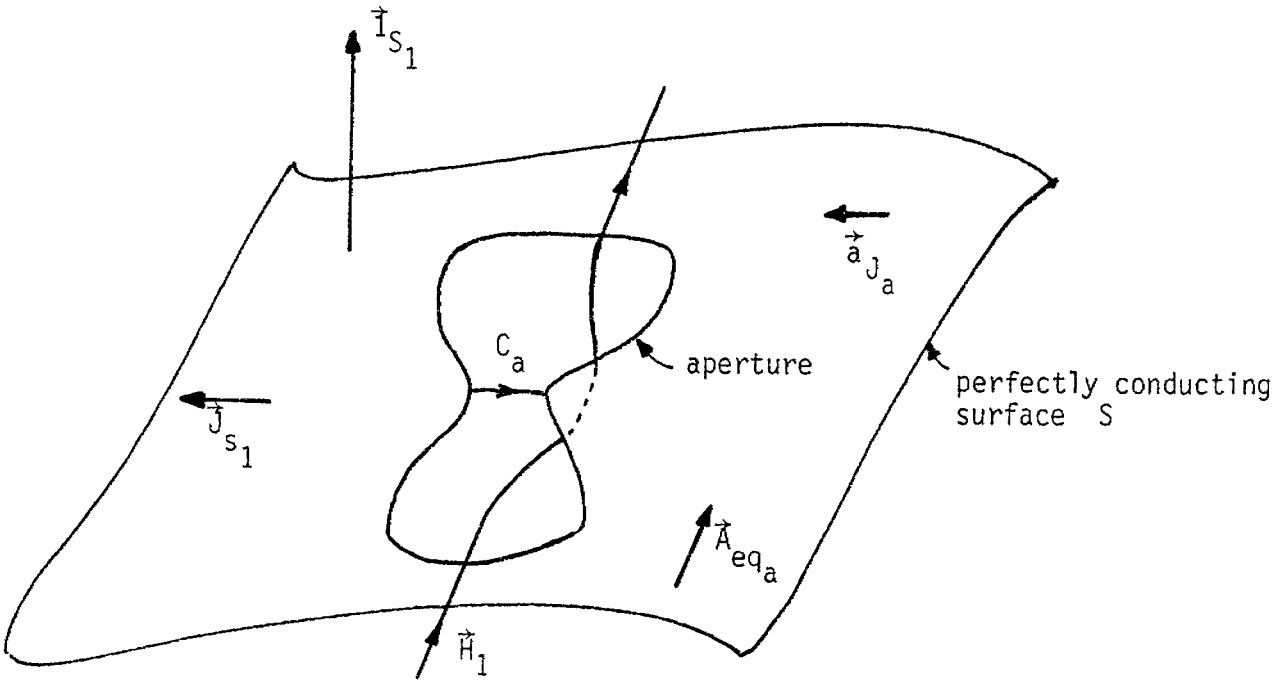

Figure 1.2 Measurement of surface magnetic fields with apertures.

$$\vec{B}_1(t) = \mu_o \vec{H}_1(t) \tag{1.3}$$

with μ_o = permeability of the assumed free space medium. In general, the actual loop design is more complex than a simple contour, involving hemi-cylinders and elaborate signal combining networks [1].

In terms of the surface current density we can use (1.1) to define

$$\begin{aligned} \vec{I}_{S_1} \times \vec{A}_{eq_\ell} &\equiv \vec{a}_{J_\ell} \\ \vec{A}_{eq_\ell} &\equiv -\vec{I}_{S_1} \times \vec{a}_{J_\ell} \end{aligned} \tag{1.4}$$

where $\vec{a}_{J_\ell}$ is an equivalent area related to the surface current density via

$$\begin{aligned} V_\ell(t) &= \mu_o \vec{A}_{eq_\ell} \cdot \frac{\partial}{\partial t} \vec{H}_1(t) \\ &= \mu_o \left[\vec{I}_{S_1} \times \vec{a}_{J_\ell}\right] \cdot \left[\vec{I}_{S_1} \times \frac{\partial}{\partial t} \vec{J}_{s_1}(t)\right] \\ &= \mu_o \vec{a}_{J_\ell} \cdot \frac{\partial}{\partial t} \vec{J}_{s_1}(t) \end{aligned} \tag{1.5}$$

or

$$\vec{a}_{J_\ell} \cdot \vec{J}_{S_1} = \frac{1}{\mu_o} \int_{-\infty}^{t} V_\ell(t')dt' \tag{1.6}$$

When there is magnetic field on only one side of the surface, an alternate way to measure the surface current density on that side is to use an aperture as the one generically shown in figure 1.2. In this measurement, the magnetic field on the side of interest is partially allowed to penetrate to the other side as indicated.

The measured quantity here is the open circuit voltage $V_{oc}(t)$ given by

$$V_{oc}(t) = -\int_{C_a} \vec{E}_1(t) \cdot d\vec{\ell} \tag{1.7}$$

where the contour C_a is indicated in figure 1.2. As before, in terms of the surface current density, we can use (1.1) to define

$$\vec{I}_{S_1} \times \vec{A}_{eq_a} \equiv \vec{a}_{J_a}$$

$$\vec{A}_{eq_a} = -\vec{I}_{S_1} \times \vec{a}_{J_a} \tag{1.8}$$

where $\vec{a}_{J_a}$ is an equivalent area related to the surface current density via

$$\begin{aligned} V_{oc}(t) &= \mu_o \vec{A}_{eq_a} \cdot \frac{\partial}{\partial t} \vec{H}_1(t) \\ &= \mu_o \left[\vec{I}_{S_1} \times \vec{a}_{J_a}\right] \cdot \left[\vec{I}_{S_1} \times \frac{\partial}{\partial t} \vec{J}_{S_1}(t)\right] \\ &= \mu_o \vec{a}_{J_a} \cdot \frac{\partial}{\partial t} \vec{J}_{S_1}(t) \end{aligned} \tag{1.9}$$

or

$$\vec{a}_{J_a} \cdot \vec{J}_{S_1}(t) = \frac{1}{\mu_o} \int_{-\infty}^{t} V_{oc}(t')dt' \tag{1.10}$$

This formally completes the description of two procedures of measuring the current density on one side of the surface, using a single loop or an aperture.

In contrast with the above, if the total current density $\vec{J}_s$ is quantity of interest, it is defined by the sum of individual current densities as

$$\vec{J}_s(t) = \vec{J}_{s_1}(t) + \vec{J}_{s_2}(t) \tag{1.11}$$

It is now observed that, in terms of the current densities both sides produce signals that add while the signals produced corresponding to the magnetic fields oppose each other, as may be seen from (1.1) and noting

$$\vec{I}_{s_1} = -\vec{I}_{s_2} \tag{1.12}$$

We may now consider three possible measurement schemes for measuring the total surface current density $\vec{J}_s(t)$ as shown in figures 1.3a, b and c. In all three figures, a single aperture is shown with integration path C_a and the open circuit voltage is proportional to the time derivative of the net or total current density. In figure 1.3a, one loop is shown and the voltage around this path vanishes, if $\vec{J}_{s_2} = \vec{J}_{s_1}$. This is seen by noting that $\vec{H}_1$ and $\vec{H}_2$ are then equal and oppositely directed, including equal distortion by the aperture. Then for a loop symmetrically positioned with respect to the conducting surface, the fluxes due to $\vec{H}_1$ and $\vec{H}_2$ cancel, giving no output. This indicates that the total current density measurement is unfeasible if we employ a single loop symmetrically positioned with respect to the conducting surface.

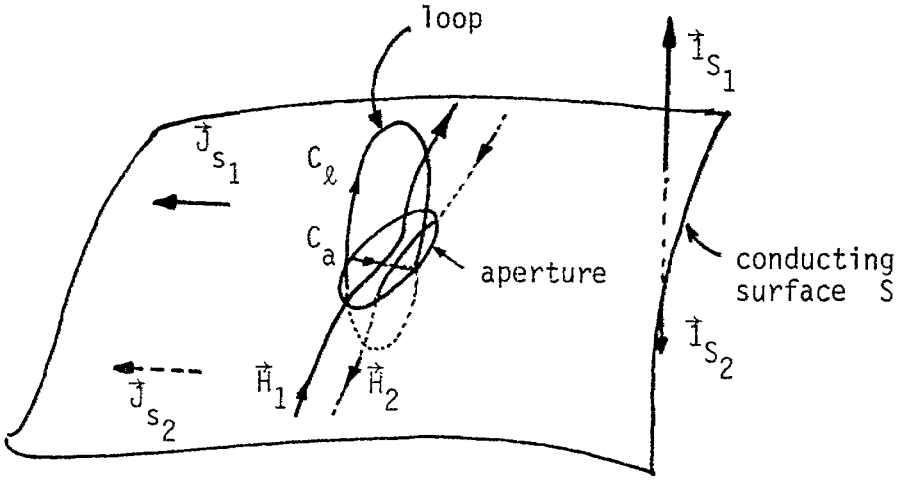

(a) use of single aperture (feasible) and a single loop (unfeasible)

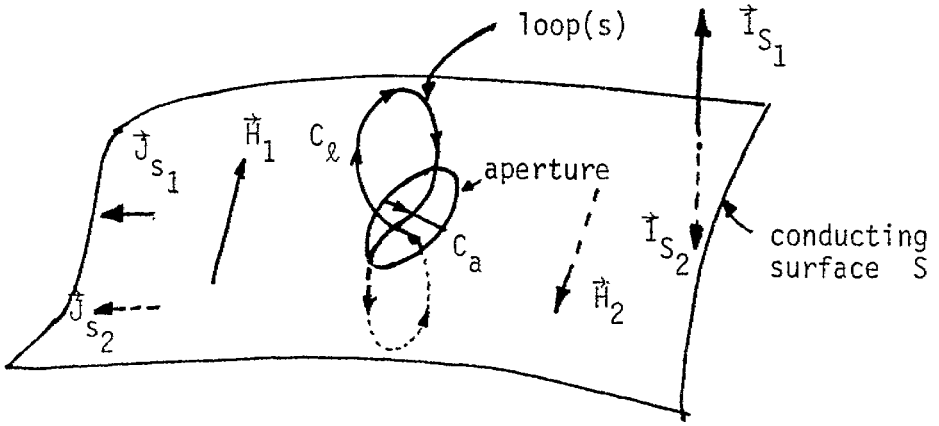

(b) use of single aperture and two loops (or one 'figure eight' loop)

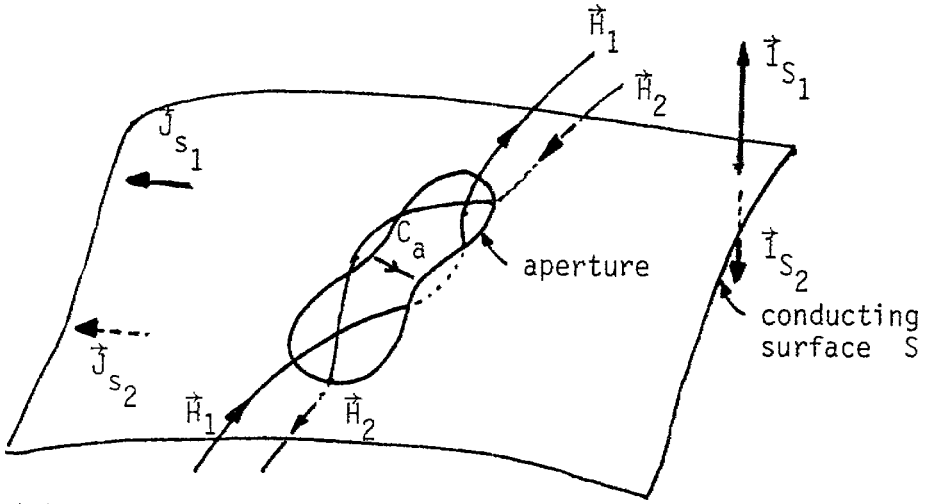

(c) use of a single aperture; detailed view

Figure 1.3 Measurement of total current density.

Such a measurement is possible if one uses two loops or one loop in the shape of a "figure 8", as shown in figure 1.3b. However, it is more easily done with a single aperture is illustrated in figure 1.3c, because of the ease of its fabrication. The governing equation for the aperture in figure 1.3c is

$$\vec{a}_{J_a} \cdot \left(\vec{J}_{s_1} + \vec{J}_{s_2}\right) = \frac{1}{\mu_o} \int_{-\infty}^{t} V_{oc}(t')dt' \qquad (1.13)$$

Note that the sum of the surface current densities is a vector sum and the case of currents flowing in opposite directions on the two sides of the conducting surface is consistent with the above expression. Some versions of such an aperture useful in measuring the total surface current density are investigated in this note.

A remark about the use of subscripts in this note is made to clarify the principal symbols. These subscripts include eq for equivalent, a for aperture, J for surface current density, d for disk, oc for open circuit, sc for short circuit, inc for incident and scat for scattered.

Some comments about the organization of this note are in order before concluding this introductory section. In Section II, aperture measurement of the surface current density is compared with the dual measurement of the normal displacement current density. In Section III, the Babinet principle for the electromagnetic fields is reviewed while relating aperture problems to disk problems, leading to complementary antennas. Section IV considers self-complementary antennas. In Sections V and VI, two examples of apertures for measuring net surface current desnity are discussed. Section VII contains a summary and is followed by a list of references.

II. Aperture Measurement of Surface Current Density Compared to Disk Measurement of Normal Displacement Current Density

In this section, we consider the problem of measuring the time rate of change of the surface current density $\vec{J}_s$ using an aperture, and an analogous measurement of $\dot{\vec{D}}$ normal to a complementary disk as indicated in figures 2.1 and 2.2. With reference to figure 2.1, the open circuit voltage $\tilde{V}_{oc_a}$ and the short circuit current $\tilde{I}_{sc_a}$ are related through the aperture impedance $Z_a (= sL_a$ as $s \to 0)$ as given by

$$\begin{aligned} \tilde{V}_{oc_a} &= \tilde{I}_{sc_a} \tilde{Z}_a \\ &= sL_a \tilde{I}_{sc_a} \qquad \text{(at low frequencies)} \end{aligned} \tag{2.1}$$

In time domain

$$V_{oc_a}(t) = L_a \frac{dI_{sc}}{dt} = L_a \vec{\ell}_{J_a} \cdot \frac{\partial \vec{J}_s}{\partial t} \tag{2.2}$$

where $\vec{\ell}_{J_a}$ is the equivalent length of the aperture. Note that equivalent areas and lengths are related through the common formula [1]

$$\vec{\ell}_{eq_a} = \frac{\mu_o}{L_a} \vec{A}_{eq_a} \quad , \quad \vec{\ell}_{J_a} = \frac{\mu_o}{L_a} \vec{A}_{J_a} \tag{2.3}$$

Similarly for the analogous measurement of the normal component of displacement current, the sensor geometry is shown in figure 2.2. It consists of a conducting disk sensing element centered in a circular aperture in a conducting ground plane [2,3, and 4]. Here the disk has a capacitance C_{disk} (as $s \to 0$) and the relationships of the sensor outputs are

$$\tilde{I}_{sc_d} = \tilde{Y}_d \tilde{V}_{oc_d} = sC_{disk} \tilde{V}_{oc_d} \tag{2.4}$$

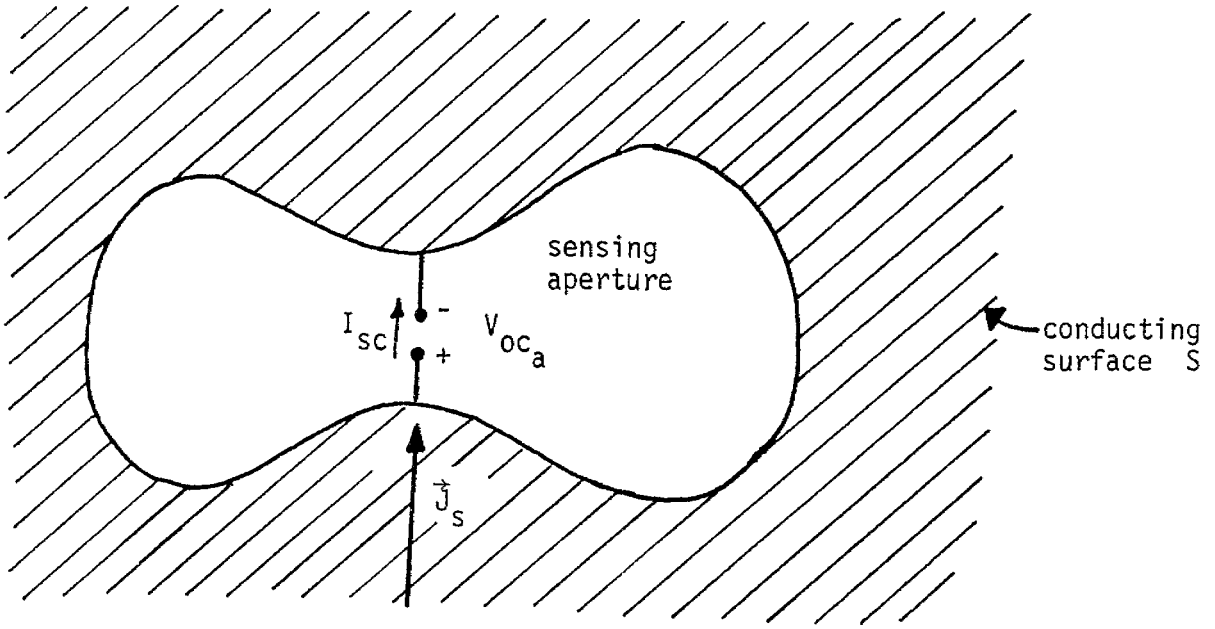

Figure 2.1. Measurement of $\vec{J}_s$ with an aperture.

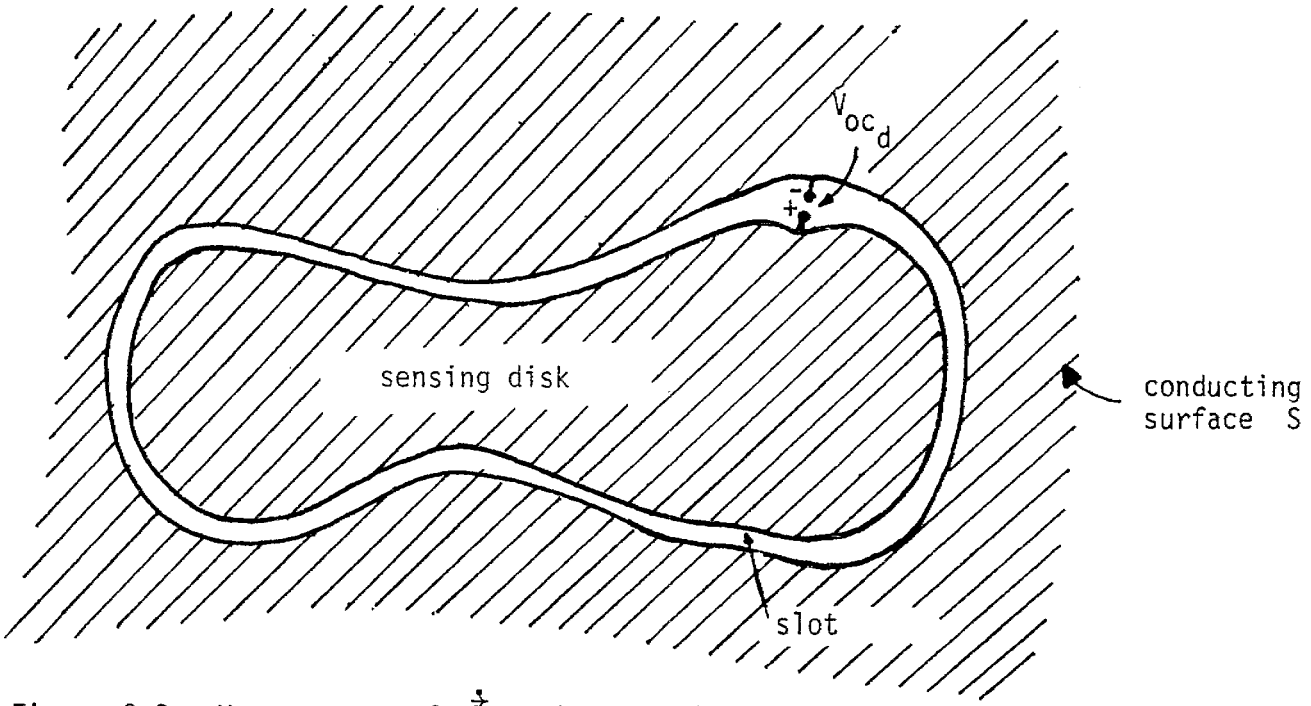

Figure 2.2. Measurement of $\vec{D}$ using a disk in a plane.

$$
\begin{aligned}
I_{sc_d}(t) &= C_{disk} \frac{dV_{oc_d}}{dt} \\
&= -A_{eq_d} \cdot \frac{\partial \vec{D}}{\partial t} \\
&= -\varepsilon_o \vec{A}_{eq} \cdot \frac{\partial \vec{E}}{\partial t} \\
&= -C_{disk} \vec{\ell}_{eq_a} \cdot \frac{\partial \vec{E}}{\partial t}
\end{aligned}
\tag{2.5}
$$

One can see the analogy in the two measurements, by comparing (2.5) and (2.2). In a manner similar to (2.3) of the aperture, we have for the disk sensor

$$
\vec{\ell}_{eq_d} = \frac{\varepsilon_o}{C_{disk}} \vec{A}_{eq_d} \tag{2.6}
$$

In concluding this section, certain observations are in order. First, note that these two measurements do not form a complementary pair in a Babinet sense, since the disk in a conducting plane is not a Babinet complement of an aperture in a conducting plane. However, the two measurements described above are dual in the sense of measuring dual electromagnetic parameters [1].

III. Review of Babinet's Principle

The Babinet principle is based on the dual nature of Maxwell's equations, i.e. the roles of electric and magnetic fields are reversed in complementary boundary value problems. Maxwell's equations in frequency domain, when charges and currents (both electric and magnetic) are present are given by [5],

$$\nabla \times \tilde{\vec{E}} = -s\vec{\mu} \cdot \tilde{\vec{H}} - \tilde{\vec{J}}_m \tag{3.1a}$$

$$\nabla \times \tilde{\vec{H}} = s\vec{\varepsilon} \cdot \tilde{\vec{E}} + \tilde{\vec{J}} \tag{3.1b}$$

$$\nabla \cdot \tilde{\vec{D}} = \tilde{\rho} \tag{3.1c}$$

$$\nabla \cdot \tilde{\vec{B}} = \tilde{\rho}_m \tag{3.1d}$$

and the continuity equations are given by

$$\nabla \cdot \tilde{\vec{J}} = -s\tilde{\rho} \tag{3.1e}$$

$$\nabla \cdot \tilde{\vec{J}}_m = -s\tilde{\rho}_m \tag{3.1f}$$

where the various quantities have their usual significance, while noting that s is the complex frequency $= \Omega + j\omega$ and the propagation constant is given by

$$\gamma = s/c \tag{3.2}$$

with c = speed of light in the general medium.

Now consider the problem of an aperture in a perfectly conducting surface in a free space medium as shown in figure 3.1. For the assumed free space medium, $\overleftrightarrow{\varepsilon}$ and $\overleftrightarrow{\mu}$ reduce to ε_o and μ_o and the fields, currents and charges are denoted by

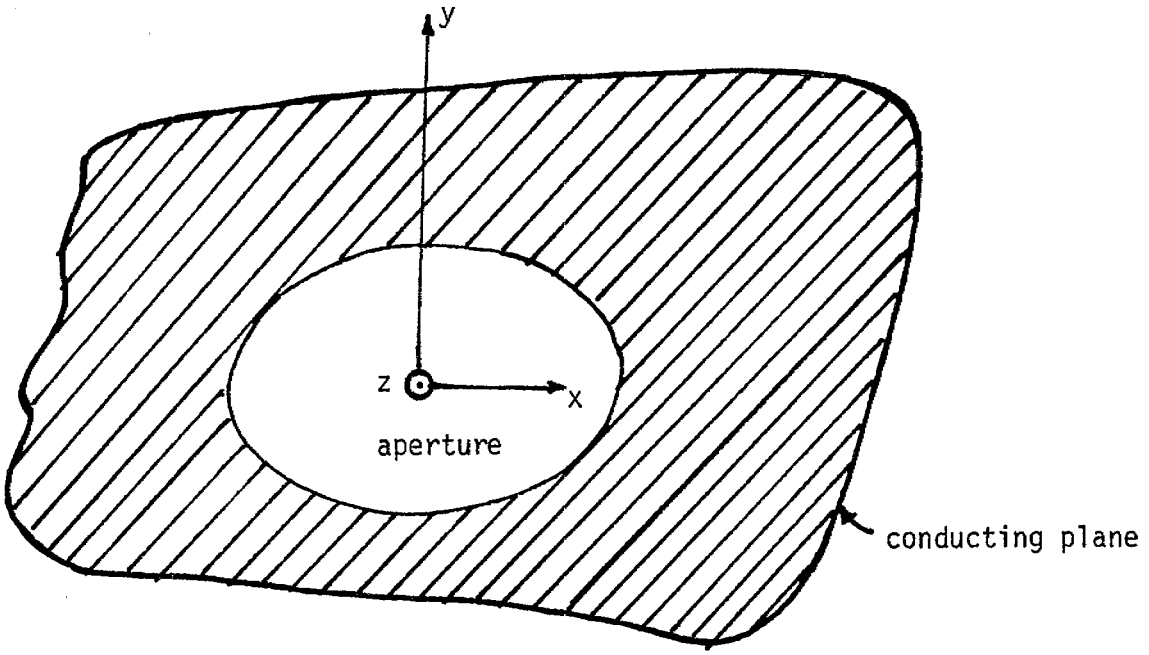

Figure 3.1 An aperture in a perfectly conducting plane.

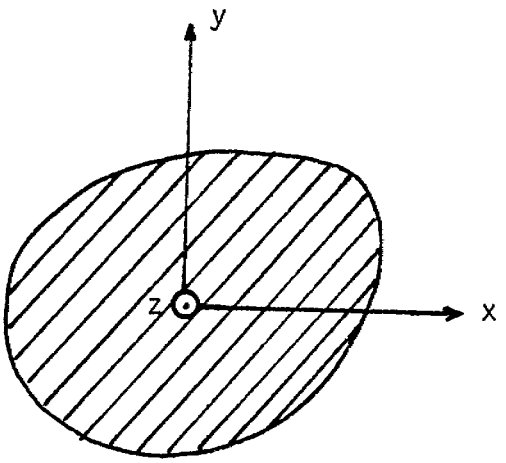

Figure 3.2 The complementary disk.

$$\tilde{\vec{E}}\ ,\ \tilde{\vec{H}}\ ,\ \tilde{\vec{J}}\ ,\ \tilde{\vec{J}}_m\ ,\ \tilde{\rho}\ ,\ \tilde{\rho}_m$$

The complementary boundary value problem [5 and 6] is indicated in figure 3.2 by interchanging apertures and conductors. So the assumed unloaded aperture in a perfectly conducting surface becomes a complementary screen problem. Let the fields, currents and charges in the complementary problem be denoted by primed quantities

$$\tilde{\vec{E}}'\ ,\ \tilde{\vec{H}}'\ ,\ \tilde{\vec{J}}'\ ,\ \tilde{\vec{J}}_m'\ ,\ \tilde{\rho}\ ,\ \tilde{\rho}_m'$$

Using the duality of Maxwell's equations, one may show the following relationships between the symmetric parts [5] of the electromagnetic quantities of the two problems. (Note that the scattered fields are purely symmetric.)

$$\tilde{\vec{E}}' = Z_o\,\tilde{\vec{H}} \qquad \text{or} \qquad \tilde{\vec{H}} = \frac{1}{Z_o}\,\tilde{\vec{E}}' \tag{3.3a}$$

$$\tilde{\vec{H}}' = -\frac{1}{Z_o}\,\tilde{\vec{E}} \qquad \text{or} \qquad \tilde{\vec{E}} = -Z_o\,\tilde{\vec{H}}' \tag{3.3b}$$

$$\tilde{\vec{J}}' = \frac{1}{Z_o}\,\tilde{\vec{J}}_m \qquad \text{or} \qquad \tilde{\vec{J}}_m = Z_o\,\tilde{\vec{J}}' \tag{3.3c}$$

$$\tilde{\vec{J}}_m' = -Z_o\,\tilde{\vec{J}} \qquad \text{or} \qquad \tilde{\vec{J}} = -\frac{1}{Z_o}\,\tilde{\vec{J}}_m' \tag{3.3d}$$

$$\tilde{\rho}' = \frac{1}{Z_o}\,\tilde{\rho}_m \qquad \text{or} \qquad \tilde{\rho}_m = Z_o\,\tilde{\rho}' \tag{3.3e}$$

$$\tilde{\rho}_m' = -Z_o\,\tilde{\rho} \qquad \text{or} \qquad \tilde{\rho} = -\frac{1}{Z_o}\,\tilde{\rho}_m' \tag{3.3f}$$

In addition to the above, potentials, impedances, admittances and boundary conditions transform in a similar manner. The transformation of boundary conditions implies that if tangential components of $\tilde{\vec{E}}$ are specified, the tangential components of $\tilde{\vec{H}}'$ are immediately known and likewise for the normal components as well. This formally completes a statement of the Babinet principle and it is noted that the Babinet principle can also be generalized to loaded apertures [5].

We may consider some characteristic equivalence between an aperture and its Babinet complement when both are used as antennas as indicated in figure 3.3. For the aperture, an integration contour C_a for the electric field is indicated resulting in a measured voltage V_{oc_a} given by

$$V_{oc_a}(t) = -\int_{C_a} \vec{E}_a \cdot d\vec{\ell} \tag{3.4}$$

Similarly, for the complementary disk, if we integrate the total magnetic field along the path C_d which circles the disk, we have

$$I_{sc_d}(t) = \oint_{C_d} \vec{H}'_{tot} \cdot d\vec{\ell} = \oint_{C_d} \vec{H}'_{sc} \cdot d\vec{\ell} \tag{3.5}$$

Observe that the above quantities of measurement are also related to the corresponding field quantities as

$$\begin{aligned} V_{oc}(t) \equiv -\int_{C_a} \vec{E} \cdot d\vec{\ell} &= \mu_o \vec{a}_{J_a} \cdot \frac{\partial \vec{J}_s}{\partial t} \\ &= \mu_o \vec{a}_{J_a} \cdot \frac{\partial \vec{J}_{s_1}}{\partial t} \quad (\text{for } \vec{J}_{s_2} = \vec{0}) \\ &= \mu_o \vec{a}_{J_a} \cdot \left[2 \vec{I}_{S_1} \times \frac{\partial \vec{H}_{inc}}{\partial t}\right] \\ &= 2\mu_o \left[\vec{I}_{S_1} \times \vec{A}_{eq_a}\right] \cdot \left[\vec{I}_{S_1} \times \frac{\partial \vec{H}_{inc}}{\partial t}\right] \quad (\text{using (1.4)}) \\ &= 2\mu_o \vec{A}_{eq_a} \cdot \frac{\partial \vec{H}_{inc}}{\partial t} \end{aligned} \tag{3.6}$$

$$I_{sc_a}(t) = \vec{\ell}_{J_a} \cdot \vec{H}_{inc}(t) \tag{3.7}$$

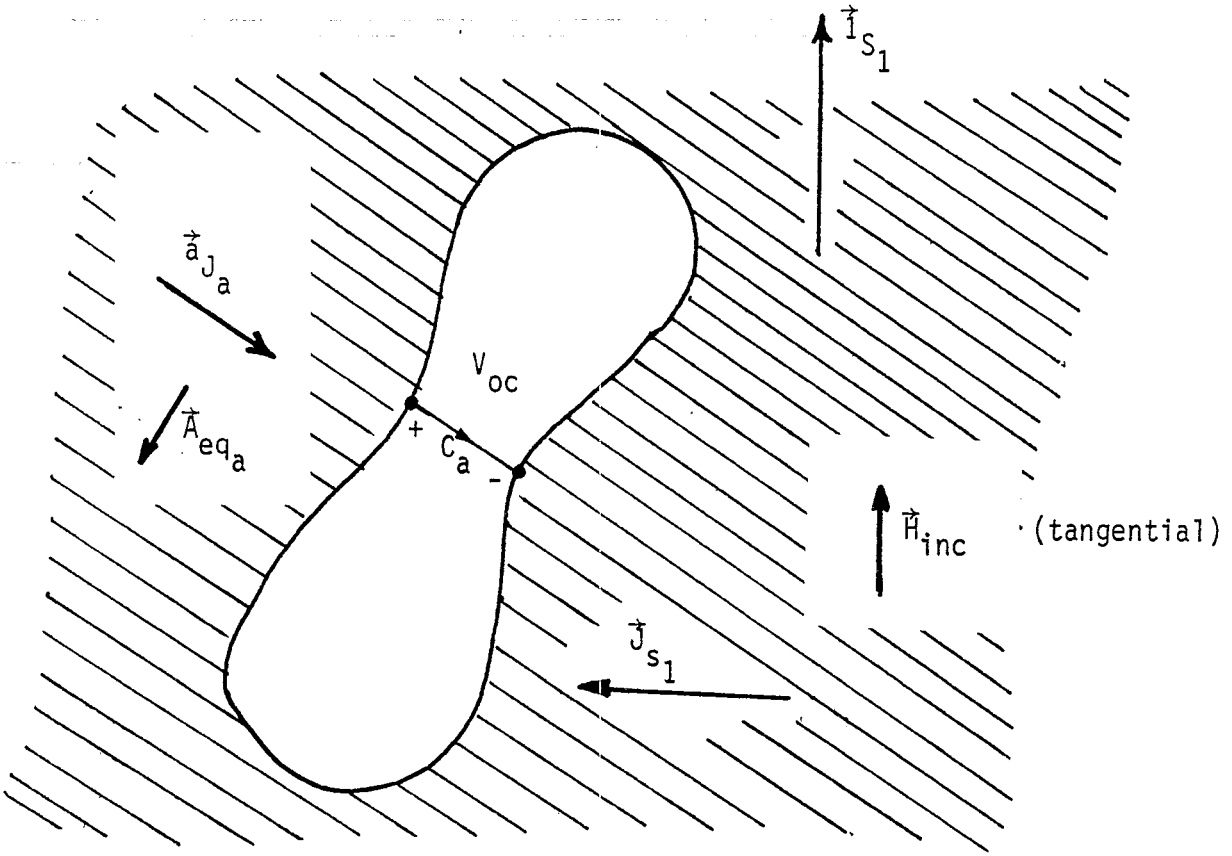

a) An aperture antenna

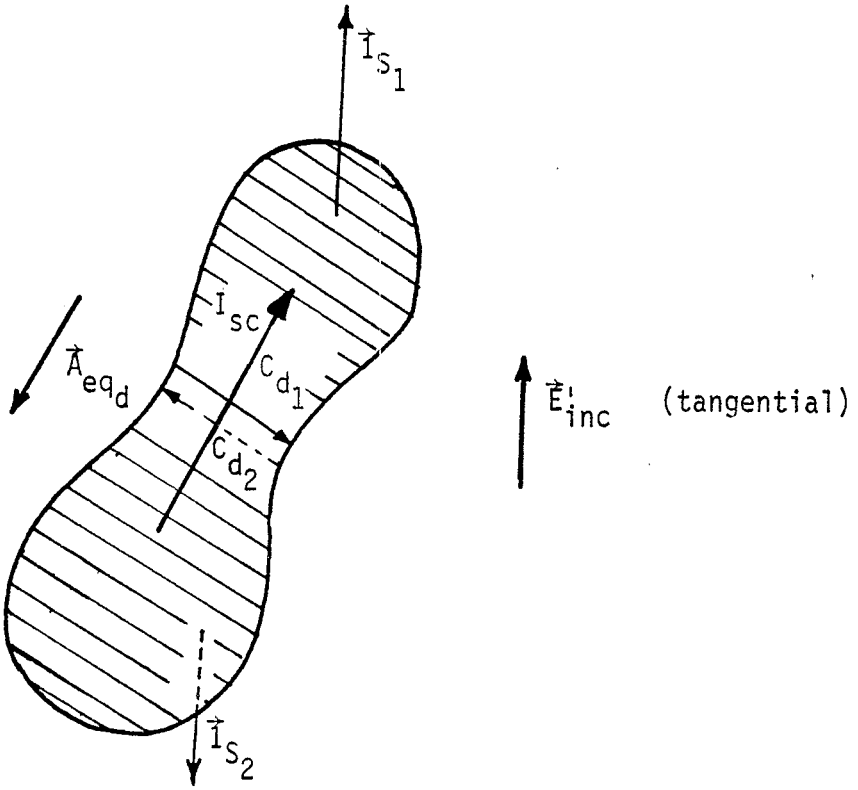

b) The complementary disk antenna

Figure 3.3. Complementary pair of an aperture and a disk used as antennas.

and for the disk

$$I_{sc_d}(t) = \oint_{C_d} \vec{H}'_{scat} \cdot d\vec{\ell} \equiv - \vec{A}_{eq_d} \cdot \left[\frac{\partial \vec{D}'_{inc}}{\partial t}\right] \tag{3.8}$$

$$V_{oc_d}(t) \equiv - \vec{\ell}_{eq_d} \cdot \vec{E}'_{inc} \tag{3.9}$$

Furthermore, $I_{sc_d}(t)$ can be related to $V_{oc_a}(t)$ as follows

$$I_{sc_d}(t) = \oint_{C_d} \vec{H}'_{scat} \cdot d\vec{\ell} = \oint_{C_{d_1}+C_{d_2}} \vec{H}'_{scat} \cdot d\vec{\ell} = 2 \int_{C_{d_1}} \vec{H}'_{scat} \cdot d\vec{\ell}$$

$$= -2 \int_{C_{d_1}} \frac{1}{Z_o} \vec{E} \cdot d\vec{\ell} = - \frac{2}{Z_o} \int_{C_a} \vec{E} \cdot d\vec{\ell}$$

$$= \frac{2}{Z_o} V_{oc_a}(t) \tag{3.10}$$

We also have from the Babinet principle [5],

$$\tilde{Z}_a \tilde{Z}_d = Z_o^2/4 \tag{3.11}$$

where

$$\tilde{Z}_a = \text{aperture impedance} = \frac{\tilde{V}_{oc_a}(s)}{\tilde{I}_{sc_a}(s)} = sL_a \quad \text{as} \quad s \to 0$$

$$\tilde{Z}_d = \text{disk impedance} = \frac{\tilde{V}_{oc_d}(s)}{\tilde{I}_{sc_d}(s)} = \frac{1}{sC_{disk}} \quad \text{as} \quad s \to 0 \tag{3.12}$$

and (3.3a and b) apply in relating the fields in the two problems. In the frequency domain (3.6) to (3.9) become

$$\tilde{V}_{oc_a}(s) = 2s\mu_o \vec{A}_{eq_a} \cdot \tilde{\vec{H}}_{inc} \quad \text{as} \quad s \to 0$$

$$\tilde{I}_{sc_a}(s) = \vec{\ell}_{J_a} \cdot \tilde{\vec{H}}_{inc} \quad \text{as} \quad s \to 0 \tag{3.13}$$

and

$$\tilde{V}_{oc_d}(s) = -\vec{\ell}_{eq_d} \cdot \tilde{\vec{E}}'_{inc} \quad \text{as} \quad s \to 0$$

$$\tilde{I}_{sc_d}(s) = -s\varepsilon_o \vec{A}_{eq_d} \cdot \tilde{\vec{E}}'_{inc} \quad \text{as} \quad s \to 0 \tag{3.14}$$

with an assumed free space medium.

But (3.10) in frequency domain also implies

$$\tilde{I}_{sc_d}(s) = \frac{2}{Z_o} \tilde{V}_{oc_a}(s) \tag{3.15}$$

or

$$-s\varepsilon_o \vec{A}_{eq_d} \cdot \tilde{\vec{E}}'_{inc} = \frac{2}{Z_o} (2s\mu_o) \vec{A}_{eq_a} \cdot \tilde{\vec{H}}_{inc} \tag{3.16}$$

Now

$$\vec{A}_{eq_a} \cdot \tilde{\vec{H}}_{inc} = \vec{A}_{eq_a} \cdot \tilde{\vec{H}}_{scat_{sc}} \tag{3.17}$$

i.e. the tangential components of incident and scattered magnetic field are the same on a shorted aperture. Since $\tilde{\vec{H}}_{scat_{sc}}$ is symmetric, we have

$$\vec{A}_{eq_a} \cdot \vec{H}_{scat_{sc}} = \frac{1}{Z_o} \vec{A}_{eq_a} \cdot \vec{E}'_{scat_{sc}} \tag{3.18}$$

but the boundary condition that tangential $\vec{E}$ on a shorted aperture be zero, gives

$$\vec{A}_{eq_a} \cdot \vec{E}'_{scat_{sc}} = - \vec{A}_{eq_a} \cdot \vec{E}'_{inc} \tag{3.19}$$

Combining the above

$$\begin{aligned} \vec{A}_{eq_d} \cdot \vec{E}'_{inc} &= - 4Z_o \vec{A}_{eq_a} \cdot \vec{H}_{inc} \\ &= 4\vec{A}_{eq_a} \cdot \vec{E}'_{inc} \end{aligned} \tag{3.20}$$

or since $\vec{E}'_{inc}$ is general

$$\vec{A}_{eq_d} = 4\vec{A}_{eq_a} \tag{3.21}$$

Using (2.3) and (2.6), (3.21) may be written as

$$\left(\frac{C_{disk}}{\varepsilon_o}\right) \vec{\ell}_{eq_d} = 4\left(\frac{L_a}{\mu_o}\right) \vec{\ell}_{eq_a} \tag{3.22}$$

or

$$\vec{\ell}_{eq_d} = \left(\frac{L_a}{C_{disk}}\right) \frac{4}{Z_o^2} \vec{\ell}_{eq_a} \tag{3.23}$$

which leads to

$$\vec{\ell}_{eq_d} = \vec{\ell}_{eq_a} \tag{3.24}$$

if we use the low frequency asymptotic form of (3.11).

Hence, knowing the equivalent areas and lengths for a disk, we also have directly the same parameters for the complementary aperture.

It is also observed that a practical realization of the complementary pair of antennas of figure 3.3 is indicated in figures 3.4 and 3.5. In both these figures terminal pairs are indicated where actual measurements of open-circuit and short-circuit parameters are made. In the case of the aperture, the measurement scheme involves a strip (or "flat" wire) whereas for the disk there is a corresponding gap. Such are the compromises needed in the practical implementation of electromagnetic concepts. If, however, the strip (or wire) is very narrow it will make no significant correction to $\vec{A}_{J_a}$, but does have a more significant effect on L_a and hence on $\vec{\ell}_{J_a}$.

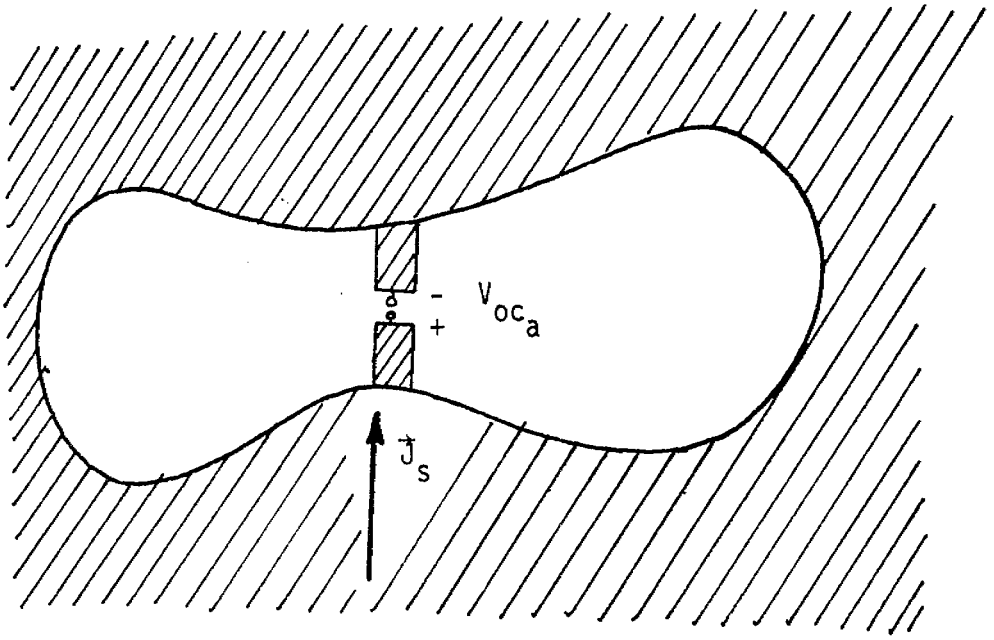

Figure 3.4. Practical realization of an aperture antenna in an infinite perfectly conducting plane.

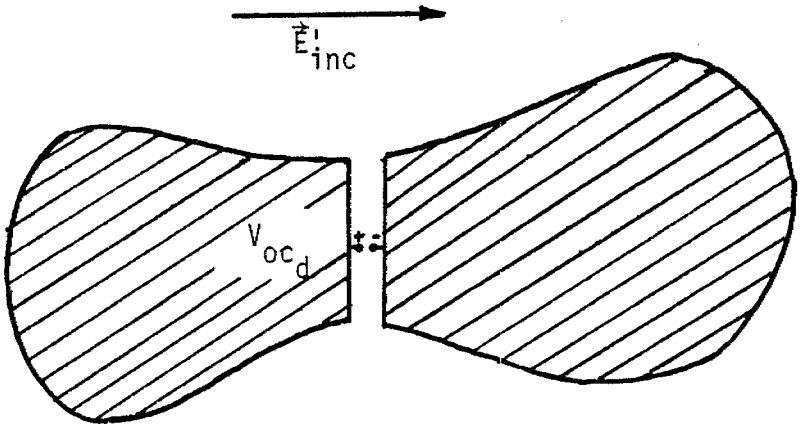

Figure 3.5. Practical realization of the complementary disk antenna.

IV. Self-Complementary Antennas

The self complementary antenna is defined as one which upon rotation in its plane by some angle (π/n where n is an integer) produces the complementary antenna. (This implies that rotation by twice this angle would preserve the geometry of the antenna.) An example is a flat 45-degree angle cone shown in figure 4.1. Figure 4.1(a) shows a flat 45-degree angle cone, whose complement is indicated in figure 4.1(b). The complementary antenna is obtained simply by interchanging apertures and conductors. It is also noted that a rotation of the antenna in figure 4.1(a) by $\pi/2$ also produces the complementary antenna. This is an example of a self-complementary antenna where the integer n above is 2.

The main feature of a self-complementary antenna is that its impedance is given by one half of the characteristic impedance of the medium. For example, if the 45-degree flat cone is surrounded by free space medium, its impedance will be $Z_o/2 \simeq 188.49\ \Omega$. This performance feature can simplify the design considerations in certain sensing or measurement applications.

There are various other shapes and loadings of self-complementary antennas [5,7], which are useful in applications requiring antenna impedances that are frequency independent over a fairly wide band.

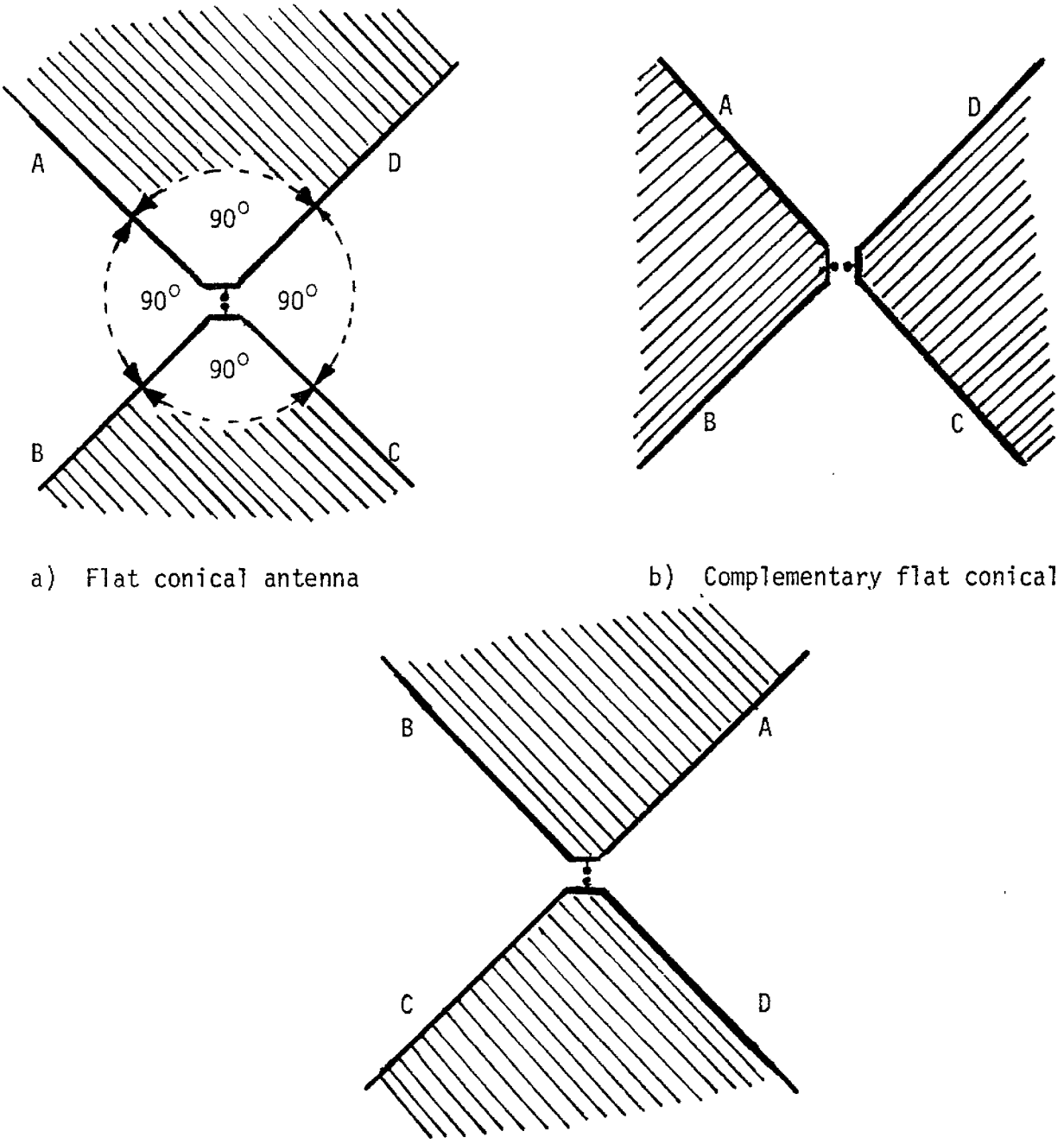

a) Flat conical antenna

b) Complementary flat conical antenna

c) After rotation by $\pi/2$

Figure 4.1. Self-complementary flat conical antenna.

V. Complementary Bow-Tie Antenna

It was shown in Section I that an aperture in a conducting surface is adequate to measure the total or net surface current density on the surface which equals the sum of the two current densities on the two sides of the surface. In this section, one such aperture in the shape of a bow-tie is investigated. Although less accurate than an elliptically shaped aperture for instance, the bow-tie aperture has its advantage in terms of speed, as discussed below.

At the outset, the impedance of the complementary bow-tie antenna is easily related to the pulse impedance of the conical antenna of figure 5.1. The complementary bow tie is shown in figure 5.2.

The pulse impedance of the conical antenna is available [8, 9] and is given by

$$Z_c = f_g Z_o \tag{5.1}$$

where f_g is a dimensionless geometric constant given by

$$f_g = \frac{K(m)}{K(m_1)} \tag{5.2}$$

with

$$\begin{aligned} m = (1 - m_1) &= \tan^4\left(\frac{\theta_o}{2}\right) \\ &= \tan^4\left[\frac{(\pi/2) - \theta_h}{2}\right] \\ &= \left[\frac{1 - \sin(\theta_h)}{\cos(\theta_h)}\right]^4 \end{aligned} \tag{5.3}$$

and $K(m)$ and $K(m_1)$ denote the complete elliptic integrals of the first kind. It is noted that some limiting forms are available [8] for special values of the angles as follows. For $\theta_o << 1$, i.e. θ_h close to $(\pi/2)$ or $m << 1$,

$$f_g \simeq \frac{\pi}{4 \ln\left[2 \cot\left(\frac{\theta_o}{2}\right)\right]} = \frac{\pi}{4 \ln\left[\frac{2 \cos(\theta_h)}{1 - \sin(\theta_h)}\right]} \tag{5.4}$$

For θ_o close to $(\pi/2)$, i.e. $\theta_h << 1$ or $m_1 << 1$,

$$f_g \simeq \frac{1}{\pi} \ln\left[\frac{16}{1 - \tan^4\left(\frac{\theta_o}{2}\right)}\right] = \frac{1}{\pi} \ln\left[\frac{16}{1 - \left\{\frac{1 - \sin(\theta_h)}{\cos(\theta_h)}\right\}^4}\right] \tag{5.5}$$

$$= \frac{1}{\pi} \ln\left[\frac{4}{\theta_h}\right] + O(\theta_h)$$

Graphs and tables of f_g for varying values of θ_o or θ_h are readily computed using the exact expressions (5.1) to (5.3) and they are available, if needed in [8 and 9].

Next we turn our attention to the input capacitance of the conical antenna, from which the inductance of the complementary bow tie is easily derived using the Babinet principle. This input

capacitance C_1 of the conical antenna is given by

$$C_1 \simeq \frac{\text{transit time}}{Z_c} = \frac{\ell}{cZ_c} = \frac{\ell}{cf_g Z_o} = \frac{\varepsilon_o \ell}{f_g} \qquad (5.6)$$

with c = speed of light in free space

Z_o = characteristic impedance of free space

ℓ = slant length of the conical antenna

Therefore, the input impedance Z_1 of the conical antenna is then

$$Z_1 = \frac{1}{sC_1} = \frac{cf_g Z_o}{s\ell} = \frac{f_g}{s\varepsilon_o \ell} \qquad (5.7)$$

By invoking the Babinet principle reviewed in an earlier section, the inductive input impedance of the complementary bow-tie antenna Z_2 of figure 5.2 is given by

$$Z_2 = sL_a = \frac{1}{Z_1}\left(\frac{Z_o}{2}\right)^2 \qquad (5.8)$$

Inserting the expression for Z_1 from (5.8), we have

$$L_a = C_1\left(\frac{Z_o}{2}\right)^2 = \frac{Z_o^2\,\varepsilon_o \ell}{4 f_g} = \frac{\mu_o \ell}{4 f_g} \qquad (5.9)$$

The above expressions for f_g, C_1 and L_a are simple and useful in designing the complementary bow-tie antennas for net surface current density measurements. Let us illustrate two example designs, one for which the pulse impedance = 50 Ω and the other being a special case of self-complementary bow-tie antenna with $\theta_o = \theta_h = 45$ degrees.

A. Complementary Bow-Tie Antenna with Pulse Impedance = 50 Ω

If the pulse impedance is taken to be 50 Ω, we have a situation where $\theta_o << 1$ corresponding to $m << 1$ and the limiting form of (5.5) becomes applicable and therefore,

$$f_g \simeq (50/376.99) \simeq 0.133 = \frac{\pi}{4 \ln\left[2 \cot\left(\frac{\theta_o}{2}\right)\right]} \qquad (5.10)$$

Solving (3.11) for θ_o, we get

$$\theta_o \simeq 0.624 \text{ degrees} \quad \text{and} \quad \theta_h \simeq 89.376 \text{ degrees} \qquad (5.11)$$

The conical antenna, then has the following design parameters.

$$C_1 = \text{capacitance} = (\varepsilon_o \ell / f_g) \qquad (5.12)$$

$$C_1' = \text{capacitance per unit slant length} = (C_1/\ell) = (\varepsilon_o / f_g) \simeq 66.48 \text{pF/m}$$

Using the earlier results of impedance relationships, we have for the complementary bow-tie antenna,

L_a = aperture inductance $\simeq \mu_o \ell/(4 f_g)$

L'_a = aperture inductance per unit slant length (5.13)

$= (L'_a/\ell) = \mu_o/(4 f_g) = 2.362\ \mu H/m$

It is easy enough to see that if the pulse impedance = 50 Ω, the e-fold rise time of the sensor equals the transit time (ℓ/c) across the sensor, as indicated below

L_a = aperture inductance = transit time x pulse impedance

$$= \frac{\ell}{c} Z_c \qquad (5.14)$$

t_r = e-fold rise time into a 50 Ω cable

$$= \frac{L_a}{50} = \frac{\ell}{c}\left(\frac{Z_c}{50}\right) \qquad (5.15)$$

So if Z_c = 50 Ω, the band width of the sensor is essentially limited by the transit time effects [10]. It may also be concluded that this is an impractical aperture antenna to build because of the small value of θ_o.

B. Example of Bow-Tie Antenna Using Self-Complementary Angle

With reference to figures 5.1 and 5.2, we choose the following parameters.

$\theta_o = \theta_h = (\pi/4)$ radians = 45 degrees

(5.16)

ℓ_1 = 2.54 cm

We then compute

$$\ell = \ell_1 \sec(\theta_h) = 3.592 \text{ cm} = 0.03592 \text{ m}$$

$$m = \tan^4(\theta_o/2) = 0.029 \Rightarrow K(m) = 1.582$$

$$m_1 = 1-m = 0.971 \Rightarrow K(m_1) = 3.155$$

$$f_g = K(m)/K(m_1) = 0.50 \quad \text{(as expected)}$$

Z_c = pulse impedance of the self-complementary bow-tie

$$= f_g Z_o = 0.5 Z_o \simeq 188.49\ \Omega \qquad (5.17)$$

L_a = aperture inductance $\simeq$ transit time x pulse impedance

$$= \frac{\ell}{c} Z_c \simeq 23 \text{ nH}$$

t_r = e-fold rise time of this sensor into a 50 Ω cable

$$= (L_a/50) \simeq 0.45 \text{ ns} \quad (\text{or 1 ns for } t_{r_{10\text{-}90}})$$

V_s = voltage pick up at the sensor terminals

$$= L_a \frac{dI}{dt}$$

$$\simeq 23 \text{ volts for } \frac{dI}{dt} = 1 \text{ Amp/ns}$$

The above design example is indicated in figure 5.3. For this example, one may also estimate the magnitude of the equivalent length of the aperture $\vec{\ell}_{J_a}$, by recalling that it is the same as the magnitude of the equivalent length of a strip (see (3.24)) as,

$$\left|\vec{\ell}_{J_a}\right| \simeq \ell \tag{5.18}$$

and similarly

$$\left|\vec{A}_{J_a}\right| = \frac{1}{4}\left|\vec{A}_{eq_d}\right| \simeq \frac{1}{4}\left(\frac{C_1}{\varepsilon_o}\right) \simeq \left(\frac{\ell^2}{4f_g}\right) \tag{5.19}$$

while noting that the above estimates are approximate.

From the example considered, it is seen that a complementary bow-tie antenna of practical dimensions can be built to possess high-speed characteristics. Yet another version of an aperture antenna suitable for net-surface-current-density measurement is the elliptical aperture antenna, especially for applications where accuracy of measurement rather than speed is a primary requirement. Such an aperture is discussed in the following section.

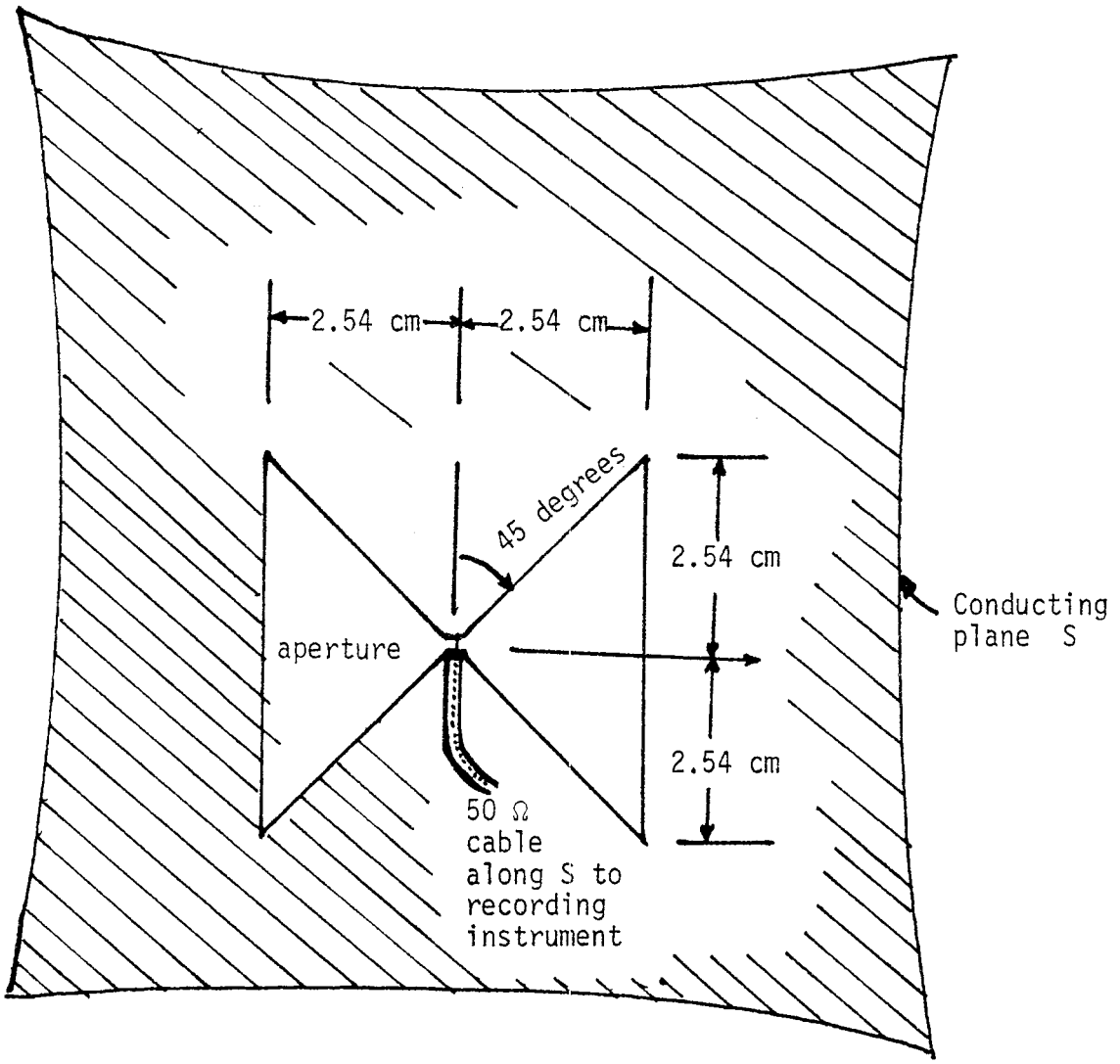

Figure 5.3 An example of a bow-tie antenna using a self-complementary angle for which the performance characteristics are estimated.

VI. Elliptic Aperture Antenna

In this section, we study an elliptic aperture antenna as it applies to the measurement of the net current density on a perfectly conducting surface. Once again Babinet's principle is useful and we may initially consider an elliptical disk antenna for the measurement of the displacement current $\vec{D}$ as indicated in figure 6.1. The disk is idealized to have zero thickness out of its plane. Two equivalent circuits [11] for this sensor are indicated in figures 6.2. The parameters of the equivalent circuit in time domain are given by

$$I_{sc_d}(t) = -\vec{A}_{eq_d} \cdot \frac{d\vec{D}}{dt}$$

$$V_{oc_d}(t) = \vec{\ell}_{eq_d} \cdot \vec{E} \qquad (6.1)$$

where the equivalent area and height are related via

$$\vec{A}_{eq_d} = \frac{C}{\varepsilon_o} \vec{h}_{eq_d} \qquad (6.2)$$

with an assumed free space medium. Detailed calculation and tabulation of the equivalent area are available [12 and 13] and a table from [13] is reproduced as table 1 here for the sake of easy reference. These references have shown that the normalized equivalent area is given by

$$\left(\frac{A_{eq_d}}{\pi ab}\right) = \frac{m}{\sqrt{1 - m}} \quad \frac{1}{K(m) - E(m)} \qquad (6.3)$$

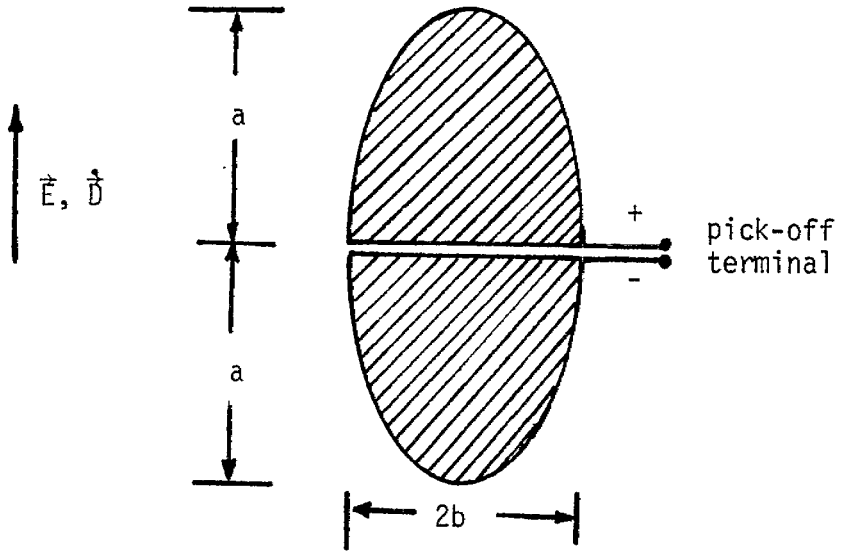

Figure 6.1 An elliptic disk $\vec{D}$ sensor, of zero thickness out of page.

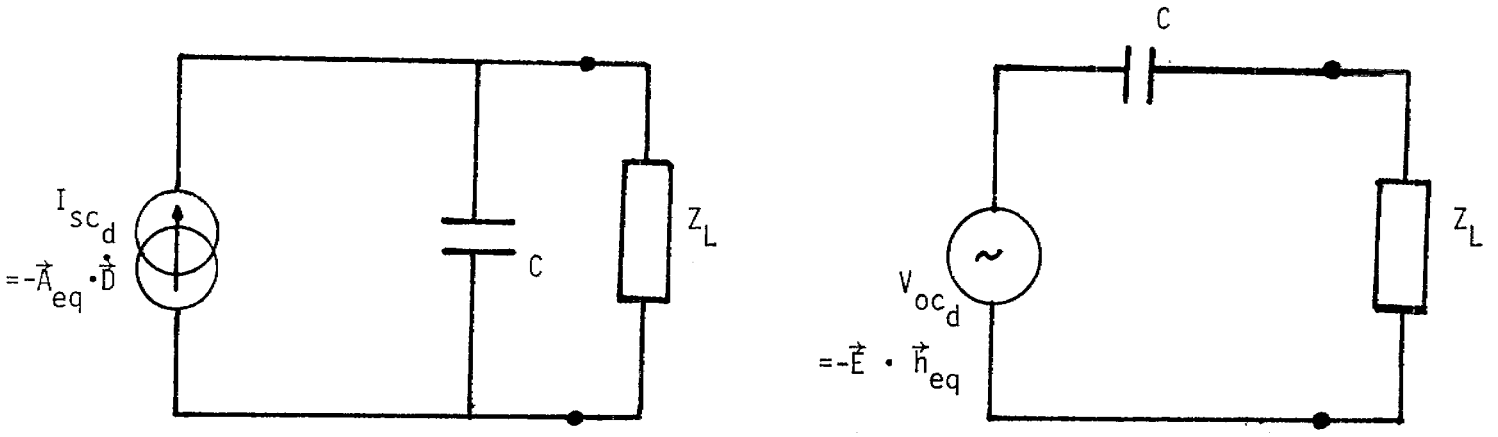

Figure 6.2 Equivalent circuits for the above elliptic disk sensor.

TABLE 6.1

NORMALIZED EQUIVALENT AREA OF AN ELLIPTIC DISK
(From [13])

b/a	$\frac{A_{eq_d}}{\pi ab}$
10^{-3}	137.0980
10^{-2}	20.0328
0.1	3.6945
0.2	2.4420
0.3	1.9890
0.4	1.7376
0.5	1.5865
0.6	1.4836
0.7	1.4091
0.8	1.3527
0.9	1.3087
1.0	1.2732

$\frac{A_{eq_d}}{\pi ab}$	$\frac{a}{b}$
1.0000	10^{-3}
1.0002	10^{-2}
1.0112	0.1
1.0324	0.2
1.0581	0.3
1.0864	0.4
1.1162	0.5
1.1469	0.6
1.1782	0.7
1.2100	0.8
1.2413	0.9
1.2732	1.0

where $m = 1 = (b^2/a^2)$ and $K(m)$, $E(m)$ are the complete elliptic integrals of the first and second kinds.

Having reviewed the elliptic disk, we may use the results previously derived on the basis of the Babinet principle, to determine the characteristic quantities for the complementary elliptic aperture. Let $\vec{A}_{eq_a}$, $\vec{\ell}_{eq_a}$, L_a represent the equivalent area, the equivalent length and the inductance of the aperture respectively. We then have

$$\vec{A}_{eq_a} = \vec{\ell}_{eq_a} \left(\frac{L_a}{\mu_o}\right) \tag{6.4}$$

with an assumed free space medium, as before.

From the Babinet principle, we have

$$\left(sL_a\right)\left(\frac{1}{sC_{disk}}\right) = \left(\frac{Z_o^2}{4}\right) \tag{6.5}$$

or

$$\left(\frac{L_a}{C_{disk}}\right) = \left(\frac{Z_o^2}{4}\right) = \left(\frac{\mu_o}{4\varepsilon_o}\right) \tag{6.6}$$

where C_{disk} is the capacitance of the disk and it has been shown earlier in (3.21) and (3.24) that the equivalent areas of the disk and aperture are simply related as

$$\begin{aligned} \vec{A}_{eq_a} &= \frac{1}{4}\ \vec{A}_{eq_d} \\ \vec{\ell}_{eq_a} &= \vec{\ell}_{eq_d} \end{aligned} \tag{6.7}$$

A. An Example of a Thin Aperture

If $(a/b) = 100$, we have from Table 6.1

$$\left(\frac{A_{eq_d}}{\pi ab}\right) = 20.0328 \tag{6.8}$$

and using (6.7)

$$\left(\frac{A_{eq_a}}{\pi ab}\right) = \frac{20.0328}{4} = 5.0082$$

$$\ell_{eq_a} = \left(\frac{\mu_o}{L_a}\right) A_{eq_a} = 5.0082\ \pi ab \left(\frac{\mu_o}{L_a}\right) \tag{6.9}$$

Therefore the net current density is derivable from

$$(\vec{H}_1 - \vec{H}_2) \cdot \vec{\ell}_{eq_a} = I_{sc_a}(t) \tag{6.10}$$

where $I_{sc_a}(t)$ is measured and ℓ_{eq_a} is estimated as outlined above

Such an elliptic aperture shown with its equivalent circuits in figures 6.3 and 6.4 can yield highly accurate measurements of the net surface current desnity, assuming that the metal is thin and that the frequency is not too low to permit the magnetic field to penetrate the metal outside the aperture. However, the bandwidth is limited by the inductance associated with the geometry of the output connection (i.e. the wire across the aperture).

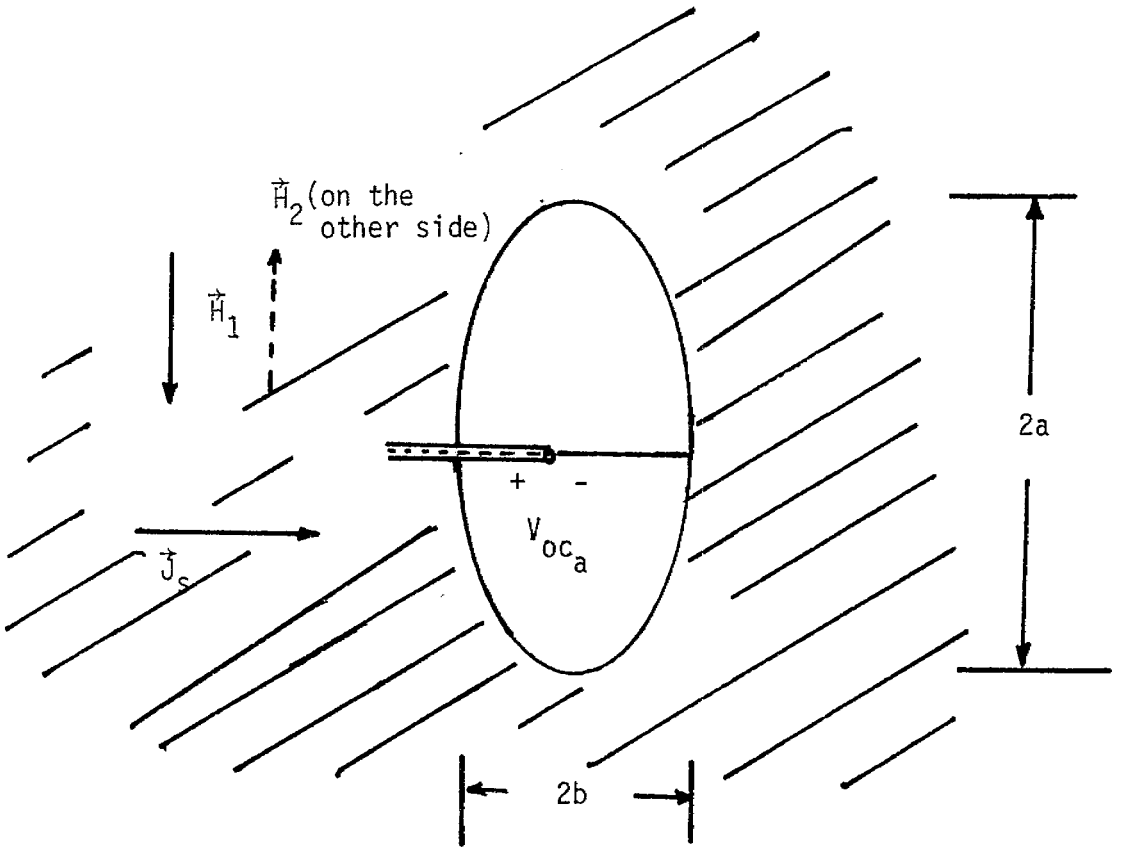

Figure 6.3 The complementary elliptic aperture antenna.

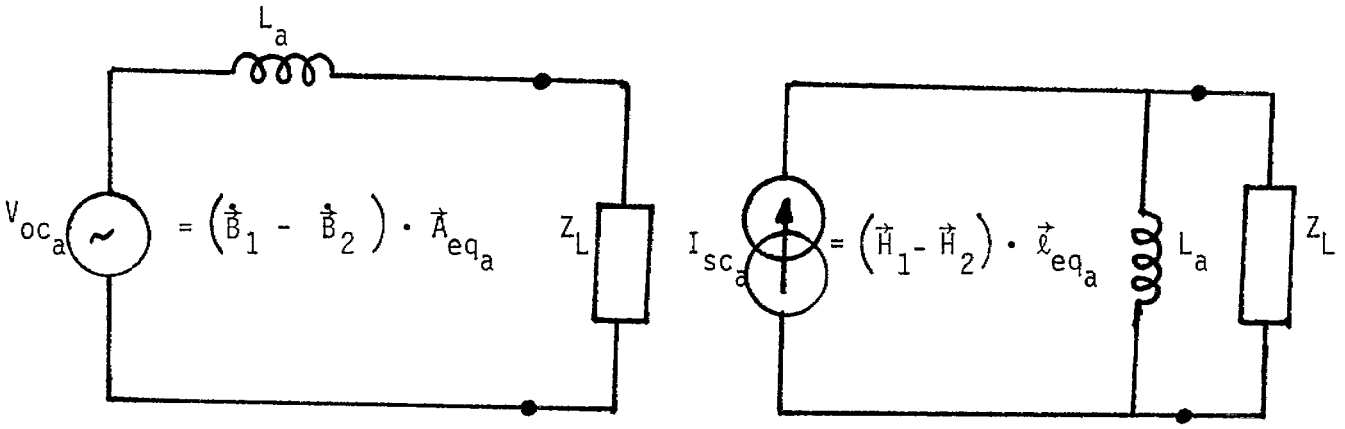

Figure 6.4 Equivalent circuits for the above complementary elliptic aperture sensor.

VII. Summary

We have addressed the problem of measuring the net surface current density on a perfectly conducting surface using apertures. Such a measurement is also possible with sensing loops on either side of the surface, while differencing their individual outputs. Apertures make this measurement simpler and two versions of such an aperture are discussed in this note.

The first version consists of a complementary bow-tie antenna, whose performance characteristics are derivable from its Babinet complement, the flat conical antenna. Such an aperture is especially suited in applications where the sensor speed is of concern. Two cases of the complementary bow-tie antenna are studied. One is the antenna with its pulse impedance equal to the pick-up coaxial cable impedance of 50 Ω (say). The main feature here is that the bandwidth of the sensor is governed by the basic limitation of transit time effects. The other bow-tie antenna studied is a special case with the half angle of the bow-tie equal to $\pi/4$ radians. A design example of this special case is presented.

While the complementary bow tie is useful when sensing speed is a primary requirement, an elliptic aperture antenna as a sensor is suitable for applications where high degree of accuracy is required. Such an elliptic aperture sensor is investigated by relating it to the elliptic disk (or blade) antenna for which detailed calculations and results are available in the literature.

In concluding this note, it is noted that all of the design equations required for fabricating such aperture sensors are reported here. These design considerations should prove useful in future applications where simple measurement of fast-rising currents or surface current densities are required.

References

1. C.E. Baum, E.L. Breen, J.C. Giles, J. O'Neill and G.D. Sower, "Sensors for Electromagnetic Pulse Measurements Both Inside and Away from Nuclear Source Regions," Sensor and Simulation Note 239, January 1978 and Joint Special Issue on the Nuclear Electromagnetic Pulse, IEEE Trans. on Antennas and Propagation, January 1978, pp 22-35, and IEEE Trans. on Electromagnetic Compatibility, February 1978, pp. 22-35.

2. C.E. Baum, "Two types of Vertical Current Density Sensors," Sensor and Simulation Note 33, 4 February 1967.

3. C.E. Baum, "The Circular Flush-Plate Dipole in a Conducting Plane and Located in Non-Conducting Media," Sensor and Simulation Note 98, 5 February 1970.

4. R.W. Latham and K.S.H. Lee, "Capacitance and Equivalent Area of a Disk in a Circular Aperture," Sensor and Simulation Note 106, May 1970.

5. C.E. Baum and B.K. Singaraju, "Generalization of Babinet's Principle in Terms of the Combined Field to Include Impedance Loaded Aperture Antennas and Scatterers," Interaction Note 217, 27 September 1974.

6. H.G. Booker, "Slot Aerials and Their Relation to Complementary Wire Aerials," Journal of IEE, III A, 1946, pp. 620-626.

7. G.A. Deschamps, "Impedance Properties of Complementary Multiterminal Planar Structures," Trans. of IRE on Antennas and Propagation, December 1959, pp. S371-S378.

8. C.E. Baum, "A Conical-Transmission-Line Gap for a Cylindrical Loop," Sensor and Simulation Note 42, 31 May 1967.

9. C.E. Baum, "Early Time Performance at Large Distances of Periodic Planar Arrays of Planar Bicones with Sources Triggered in a Plane Wave Sequence," Sensor and Simulation Note 184, 30 August 1973.

References (concluded)

10. C.E. Baum, "Maximizing Frequency Response of a $\dot{B}$ Loop," Sensor and Simulation Note 8, 9 December 1964.

11. C.E. Baum, "Parameters for Some Electrically-Small Electromagnetic Sensors," Sensor and Simulation Note 38, 21 March 1967.

12. K.S.H. Lee, "Electrically-Small Ellipsoidal Antenna," Sensor and Simulation Note 193, February 1974.

13. K.S.H. Lee, Editor, "EMP Interaction: Principles, Techniques and Reference Data (A Compleat Concatenation of Technology from the EMP Interaction Notes) EMP Interaction 2-1," Air Force Weapons Laboratory, Kirtland AFB, NM, December 1980, pp. 391-394.

☆U.S. GOVERNMENT PRINTING OFFICE: 1985–676-135/20525